ARTICLE

The relationship between reactivity patterns of methoxyphenol positional isomers towards hydrogen-transfer reactions and their interactions at the liquid-solid interface of RANEY® Ni as probed by ATR-IR spectroscopy

Received 00th January 20xx,
Accepted 00th January 20xx

DOI: 10.1039/x0xx00000x

www.rsc.org/

Ilton Barros Daltro de Castro,[a] Inês Graça,[b] Laura Rodríguez-García,[c] Marco Kennema,[a] Roberto Rinaldi *,[b] and Fabian Meemken *,[c]

In the valorisation of lignin, the application of catalytic hydrogen transfer reactions (e.g. in catalytic upstream biorefining or lignin-first biorefining) has brought renewed interest in the fundamental understanding of hydrogen-transfer processes in the defunctionalisation/conversion of lignin-derived phenolics. In this report, we address fundamental questions underlining the distinct reactivity patterns of positional isomers of guaiacol in presence of RANEY® Ni and 2-PrOH. We studied the relationship between reactivity patterns of 2-, 3- and 4-methoxyphenols and their interactions at the liquid-solid interface of RANEY® Ni as probed by attenuated total reflection-infrared (ATR-IR) spectroscopy. Regarding the reactivity patterns, 2-methoxyphenol or guaiacol is predominantly converted into cyclohexanol through a sequence of reactions including demethoxylation of 2-methoxyphenol to phenol followed by hydrogenation of phenol to cyclohexanol. By contrast, for the conversion of the two non-lignin related positional isomers, the corresponding 3- and 4-methoxycyclohexanols are the major reaction products. To shed light on the substrate-surface interactions, the liquid-solid interface of the catalyst was examined by ATR-IR spectroscopy. We found that 2-methoxyphenol assumes a rather flat adsorption configuration on the surface of the catalyst, which allows a stronger interaction of the methoxy C—O bond with the catalyst, owing to its parallel orientation to the surface. In contrast, the adsorption of 3- or 4-methoxyphenol leads to a tilted surface complex in which the ring saturation is more favoured. In a broader context, the current results provide in-depth mechanistic insight into the H-transfer demethoxylation of phenols. As this reaction takes place under low severity conditions (i.e. 80-120ºC, autogenous pressure) and employs a non-expensive catalyst (RANEY® Ni), in-depth understanding of mechanisms underlining the product selectivity contributes to the elaboration of chemocatalytic strategies for the funnelling of lignin products (e.g. S and G → H-derived products, where 'S', 'G' and 'H' stand for syringyl, guaiacyl and coumaryl alcohol-derived products, respectively) to the corresponding demethoxylated cyclohexanols.

Significance Statement

The fundamental knowledge on how to direct product selectivity based on molecular understanding of interactions between substrate and catalyst surface is of extreme importance for the biorefinery concept. In fact, it contributes to the design of catalysts for the target production of value-added chemicals in which the problem posed by the formation of (complex) product mixtures must be alleviated, in order to improve the atom-economy of the overall process chains.

Introduction

Catalytic hydrogen transfer reactions (i.e. hydrogenation – HYD, hydrogenolysis – HYL, demethoxylation – DMO, and hydrodeoxygenation – HDO) have recently emerged as a promising pathway for biomass valorisation.[1-8] From the catalytic upstream biorefining, in which a well-defined pulp and depolymerised lignin stream are obtained, to the downstream processing of these fractions,[4,9-12] H-transfer reactions in the presence of a liquid organic H-donor have demonstrated several advantages over conventional hydrogenation in the presence of molecular hydrogen.[5] The use of liquid organic H-donors instead of H_2 enables a considerable degree of control over the reaction in terms of selectivity for given products.[5,13] In fact, organic H-donors could transfer hydrogen through different mechanistic pathways to the substrate (e.g. hydride transfer or direct hydrogen transfer also known as Meerwein–Ponndorf–Verley mechanism) and compete with the reactants and intermediates

[a] *Max-Planck-Institut für Kohlenforschung, Mülheim an der Ruhr, D-45470, Germany.*
[b] *Department of Chemical Engineering, Imperial College London, SW7 2AZ London, United Kingdom. E-mail: rrinaldi@ic.ac.uk*
[c] *Department of Chemistry and Applied Biosciences, ETH Zürich, 8093 Zürich, Switzerland. E-mail: fabian.meemken@chem.ethz.ch*
† Electronic Supplementary Information (ESI) available: See DOI: 10.1039/x0xx00000x

for the active centres on the catalyst, changing the typical product distributions.[5,6]

Hydrogen transfer reactions have been performed on several Pd, Pt, Ru, Au and Ni-based heterogeneous catalysts using different biomass-derived substrates (furans, alcohols, acids, phenols, aromatics, etc.).[4-7,14-21] In particular, the study of the phenolic molecules HDO have attracted researchers' attention in recent years due to advances in the liquid phase catalytic valorisation of lignin into high-value products.[6,7,22] Despite the refractory nature of some phenolic molecules to undergo hydrogenation in the presence of molecular hydrogen,[23,24] promising results have been found for the hydrodeoxygenation of bio-based phenols over Raney® Ni under unusual low-severity conditions (80-120°C), employing 2-propanol as an H-donor and solvent.[6] Moreover, when compared to the conventional reductive catalytic processes, this catalyst shows the ability to defunctionalise aromatic compounds through stepwise H-transfer reactions.[6] Shown in Scheme 1 is the defunctionalisation pathway of 2-methoxyphenol in the presence of Raney® Ni and 2-propanol (H-donor).

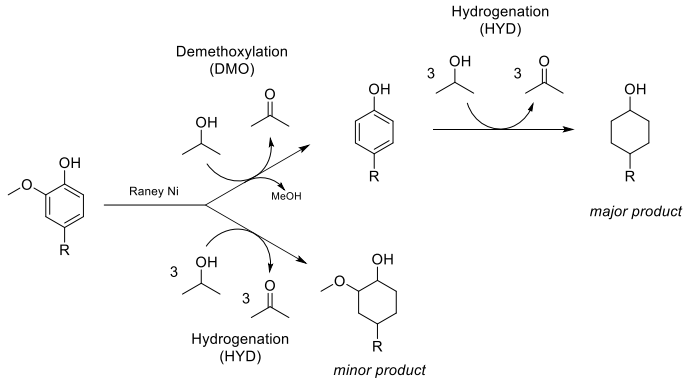

Scheme 1. Reactions proposed for the conversion of 2-methoxyphenol in the presence of Raney® Ni/2-PrOH.[6]

The conversion of 2-methoxyphenol involves firstly the DMO of the phenolic substrate, which is followed by the HYD of the phenolic intermediate to the corresponding cyclohexanol. Conversely, under H_2 pressures, the major reaction product is 2-methoxycyclohexanol,[23,25] which is formed at very low yields through the tandem H-transfer process.[6] In addition, it was verified that with Raney® Ni/2-PrOH systems 2-methoxyphenol more easily undergoes DMO under low low-severity conditions than dehydroxylation of phenol. This reactivity pattern is surprising considering that both C—O bonds in C_6H_5-OCH_3 and C_6H_5-OH present similar high values of dissociation enthalpy (385.6 and 448.4 kJ mol^{-1}, respectively).[11]

Studies using either the *meta*- or *para*-isomer as model compounds have been rather scarce in the literature, most likely because these structures are not primarily found in lignin itself.[10] However, differences in the steric constraints of the methoxy group in the various structural isomers could influence their adsorption on the catalyst surface and significantly affect the reaction, providing key information on the mechanism underlining the H-transfer demethoxylation of lignin-derived phenols.[22,26-30] Therefore, a systematic study of the three substituted methoxyphenols seems to be crucial to understand the H-transfer processes catalysed by the Raney® Ni /2-PrOH system.

In this report, we address the relationship between the reactivity of the different methoxyphenol positional isomers during H-transfer reactions on RANEY® Ni and their preferential adsorption geometry on the complex surface of this catalyst. The results and discussion is organised as follows. In the first section, the reactivity pattern for the positional isomers of methoxyphenol towards H-transfer reactions in the presence of RANEY® Ni and 2-PrOH (H-donor and solvent) was analysed based on the evolution of the product distribution. Subsequently, conventional hydrogenation of methoxyphenol isomers was carried out under H_2 pressure in 2-methyltetrahydrofuran (a non-H-donor solvent). Differences in the product distribution between conventional hydrogenation and H-transfer reaction were investigated. Furthermore, to further examine the distinct reactivity pattern of 2-methoxyphenol, H-transfer reactions were also applied to 1,2-dimethoxybenzene and 2-ethoxyphenol under the same experimental conditions. Finally, the interactions of the isomers adsorbed on Raney® Ni at the catalytic solid-liquid interface were examined by ATR-IR spectroscopy. The surface spectra reveal key features distinguishing the adsorption geometry of 2-methoxyphenol compared against the other two isomers. Overall, this paper aims at providing fundamental knowledge for the development of process options directed towards the chemo-catalytic funnelling of lignin-derived phenols into target platform chemicals for the monetisation of lignin streams.

Results and discussion

Reactivity profile of the positional isomers of methoxyphenol

Figure 1 presents the evolution of the reaction mixture composition as a function of time for the experiments performed on the positional isomers of methoxyphenol in the presence of Raney® Ni and 2-PrOH (solvent and H-donor). To better evaluate the selectivity towards hydrogenation or hydrogenolysis, the experiments were firstly performed at 80°C (Figure 1A, 1B and 1C). The conversion of 2-methoxyphenol is faster than the transformation of the other two positional isomers. Furthermore, 2-methoxyphenol is mainly converted to phenol via DMO. In sequence, the hydrogenation of phenol into cyclohexanol confirms phenol as the key intermediate in this process (Figure 1A). By contrast, the conversion of the other positional isomers of methoxyphenol rendered the corresponding methoxycyclohexanol counterparts as the major components of the reaction mixture (at 2h, 45-50%, Figure 1B and 1C). These products stem from the direct substrate saturation. Indeed, these reactions show only a slight formation of phenol throughout the reaction duration (Figure 1B and 1C). Cyclohexanol arises at the beginning of the reaction, and its concentration gradually increases to 25 mol%, in both cases, after 2h.

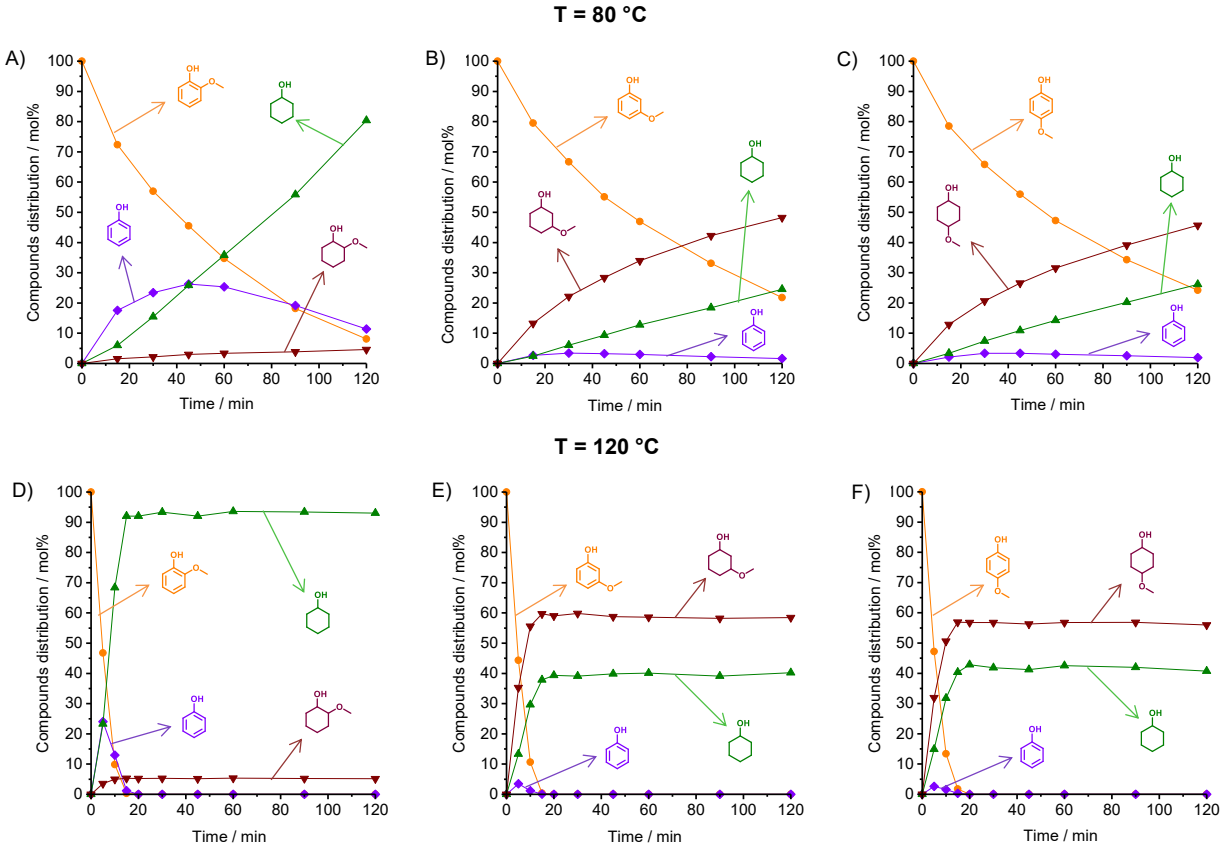

Figure 1. Distribution of compounds for the reaction at 80 and 120°C of A and D) 2-methoxyphenol, B and E) 3-methoxyphenol and C and F) 4-methoxyphenol. *Reaction conditions*: 1.8 mmol substrate, 1g RANEY® Ni (washed with 3 x 1 mL 2-PrOH), 6 mL 2-PrOH, 2h.

At 120°C, full conversion of all methoxyphenols is achieved in less than 20 min (Figure 1E-F). The reactivity profile observed for the substrates in the experiments confirms that DMO in the case of 2-methoxyphenol conversion is much more favourable than the substrate saturation to the 2-methoxycyclohexanol. Again, for the other positional isomers, the mixtures of the corresponding methoxycyclohexanol isomer and cyclohexanol (~60:40, mol/mol) was obtained. In these cases, this finding demonstrates that DMO and HYD proceed by parallel, competing pathways. Nonetheless, HYD is slightly favourable than DMO when starting from the 3- or 4-methoxyphenol. Finally, no cyclohexanone derivatives were detected in both experiment sets, indicating that the preferential H-donor is 2-propanol (i.e. the solvent). This observation is expected since 2-PrOH (solvent and H-donor) is present in a large excess of 40 equivalents relative to the substrate. Hence, the reaction is set to be pseudo-zero order in terms of 2-PrOH.

To obtain further information on the kinetics of the conversion of methoxyphenol positional isomers, a kinetic description of the reaction network for the conversion of isomers was developed, by fitting global rate expressions to the considered reaction pathways HYD and DMO of Scheme 1. Firstly, hydrogenation was performed at 80°C using different concentrations of the substrate to determine the reaction order (Supporting information, Figure S1). The conversion of the positional isomers was found to be zero order with regards to the substrate concentration in all reactions investigated in this work. This finding indicates that an Eley-Rideal mechanism is not observed in the H-transfer conversion of methoxyphenols. Otherwise, the substrate must be adsorbed on the surface to undergo the H-transfer process. Moreover, Arrhenius plots were obtained based on the measured rate at different temperatures (Supporting information, Figure S2). The Arrhenius plots indicated the activation energies of 74.6 ± 3.3, 79.7 ± 2.6 and 78.9 ± 3.6 kJ mol^{-1} for 2-methoxyphenol, 3-methoxyphenol and 4-methoxyphenol, respectively (Table 1).

Table 1. Kinetic parameters based on the Arrhenius equation for the H-transfer conversion of 2-methoxyphenol (2-MeOPh), 3-methoxyphenol (3-MeOPh) and 4-methoxyphenol (4-MeOPh).

Parameters	2-MeOPh	3-MeOPh	4-MeOPh
E_a (kJ mol^{-1})	74.6 ± 3.3	79.7 ± 2.6	78.9 ± 3.6
A (min^{-1})	(2.2 ± 0.1) ×10^9	(8.6 ± 0.4) ×10^9	(6.5 ± 0.4) ×10^9

Hydrogenation under H_2 pressure

In conventional hydrogenations under H_2 pressure, RANEY® Ni typically exhibits a higher activity than in transfer hydrogenation employing an organic molecule as a hydrogen donor.[31-33] In addition, when performing a conventional hydrogenation in a hydrogen donor solvent, a synergism in the

conversion of diphenyl ether between the two hydrogenation routes (via H_2 gas and H-transfer) was observed.[33] To examine differences in product distribution between conventional hydrogenation and H-transfer reactions at full conversion, experiments were carried out on the methoxyphenol positional isomers under H_2 pressure in 2-methyltetrahydrofuran, a non-H-donor solvent. Interestingly, reactions performed under pressure of H_2 showed for all the substrates much higher yields of methoxycyclohexanols when compared to H-transfer reactions under similar conditions (Table 2). This is especially evident for the 2-methoxyphenol as almost similar amounts of cyclohexanol (54%) and 2-methoxycyclohexanol (46%) were formed under H_2 pressure. In contrast, by H-transfer, cyclohexanol was by far the dominant product (95%). These results suggest that the overall contribution of the HYD for the final product distribution is more significant in reactions conducted under H_2 pressure. However, in the case of the 2-methoxyphenol, DMO also appears to be an important pathway regardless of the hydrogen source. This observation ignites a question whether the presence of the substituent in *ortho*-position could cause steric and/or electronic constraints, interfering with the substrate adsorption on the catalyst.

H-transfer reactions of 1,2-dimethoxybenzene and 2-ethoxyphenol

To shed light on the role of substitution on the *ortho* position, H-transfer reactions were applied to 1,2-dimethoxybenzene and 2-ethoxyphenol, using the same experimental conditions. For 1,2-dimethoxybenzene, no significant transformation occurred at 80°C, only with a very slight amount of substrate being converted into anisole (Figure 2A), in agreement with previous research.[6] In the case of the 2-ethoxyphenol (Figure 2B), despite the reaction being slower than that of the 2-methoxyphenol, the same reactivity pattern was observed. Initially, the cleavage of the ethoxyl group occurs, followed by phenol saturation, yielding cyclohexanol.

Table 2. Results of hydrogenation of 2-methoxyphenol (2-MeOPh), 3-methoxyphenol (3-MeOPh) and 4-methoxyphenol (4-MeOPh) under molecular H_2. Comparison with H-transfer results. Reaction conditions: 1.8 mmol substrate, 1g Raney® Ni, 6 mL 2-MeTHF, H_2 (40 bar pressure), 120°C, 2h.

Positional isomer	Conversion (%)	Cyclohexanol (%)		Methoxycyclohexanol isomers (%)	
		H-transfer	H_2	H-transfer	H_2
2-MeOPh	100	95	54	5	46
3- MeOPh	100	40	11	60	89
4- MeOPh	100	45	5	55	95

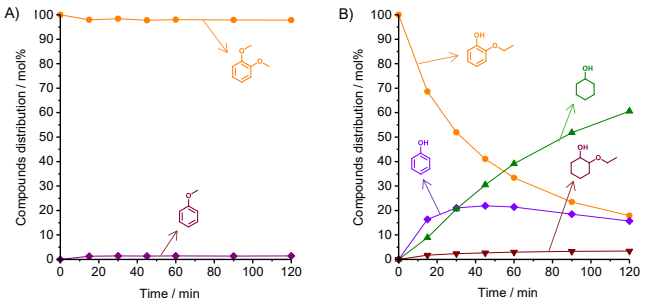

Figure 2. Distribution of compounds for the reaction with A) 1,2-dimethoxybenzene, and B) 2-ethoxyphenol in the presence of Raney® Ni/2-PrOH at 80°C, for 2h.

ATR-IR spectroscopy

The pieces of evidence presented in the previous sections indicate that the presence of the phenol group plays an important role in the interaction between the substrate and the catalytic surface. In several single crystal and density functional theory (DFT) studies, the adsorptions of phenol[22,30,34,35] on Ni and 2-methoxyphenol[27-30,36] on transition metals were investigated, and their chemisorption on RANEY® Ni was proposed to involve the aromatic ring. Furthermore, gas-phase studies on a Ni(111) surface have shown that the energy required to cleave the O—H bond of phenol is small compared to the energy required for its initial adsorption.[22,35,37] Moreover, regarding the activation of the C—O bond of the methoxy substituent on the phenolic ring, the DMO pathway is clearly favoured when the methoxy group is located at *ortho* position, compared to the *meta* and *para* positions. For the conversion of 2-methoxyphenol on Ni catalysts, steric constraints arising from the presence of the methoxy substituent at *ortho* position were suggested to play an important role to direct the reaction selectivity.[30] Recently, gas-phase intramolecular structural dynamics investigations involving methoxyphenol isomers showed that the rotational barrier of the OH substituent in 2-methoxyphenol is significantly higher than that of 3- and 4-methoxyphenol in their ground states.[38] The high rotational barrier for the 2-methoxyphenol was found to be the result of an intramolecular hydrogen-bond established between the OH group and the methoxy group, resulting in a rotation of the methoxy group out of the plane of the ring by up to 13.5°.[38]

Recently, we have studied the adsorption of phenol on RANEY® Ni in presence of cyclohexane as the solvent at 40°C.[39] This study successfully revealed key features of co-adsorption of phenols, alcohols and polyols on the complex surface of this catalyst. Therefore, to provide in-depth insight into the impact of the position of the methoxyl substituent on the adsorption geometries, and their relationships with the selectivity towards H-transfer DMO, we examined the adsorption of the positional isomers at the catalytic solid-liquid interface employing ATR-IR spectroscopy.

In Figure 3, the spectra of phenol (A) and of the three methoxyphenols (B, C, and D) dissolved in the solvent cyclohexane (grey spectra) and adsorbed on RANEY® Ni in the presence of the solvent cyclohexane (bold black spectra) at 40°C are presented. The surface spectra contain information on the molecular orientation of the detected adsorbates on the

paramagnetic metal catalyst[40] and the interaction of the phenols with RANEY® Ni. Compared to the spectra of dissolved phenols, which were recorded in the absence of catalyst at the same liquid-phase concentration (1 mM solutions), several vibrational modes are red-shifted and show different intensities, indicating the participation of the corresponding molecular moieties in the surface interaction(s).

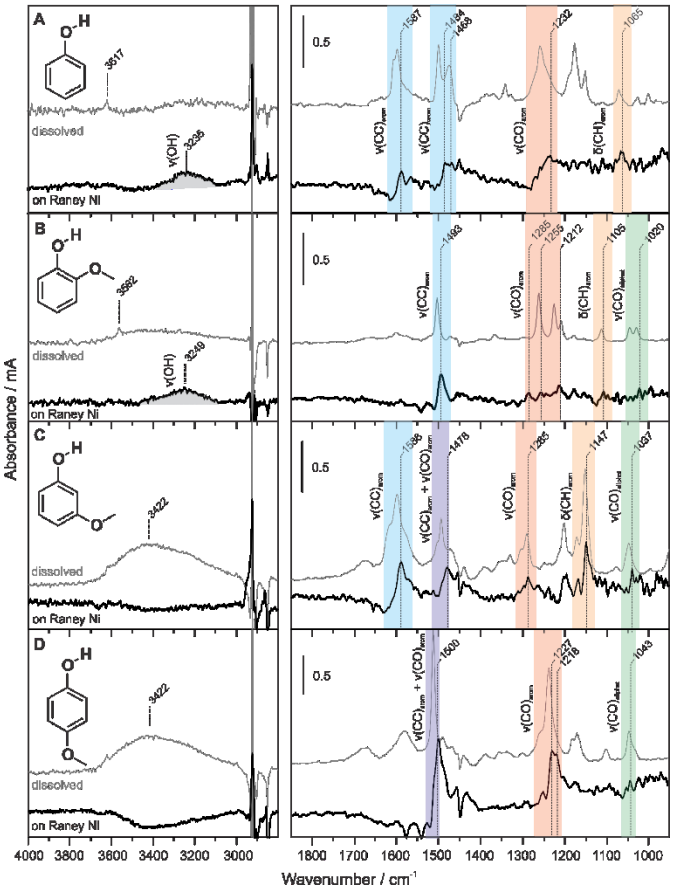

Figure 3. ATR-IR surface spectra (bold black) of phenol (A), 2-methoxyphenol (B), 3-methoxyphenol (C) and 4-methoxyphenol (D) adsorbed from a 1 mM cyclohexane solution onto RANEY® Ni at 40°C. For the sake of comparison the spectra of dissolved phenol and methoxyphenols recorded in the absence of catalyst with the same solutions are also included (grey, scaled by 0.5). The background spectrum was recorded in the presence of the solvent cyclohexane prior to admission of the methoxyphenols.

Aided by DFT gas-phase calculations, the vibrational modes of the four phenolic compounds were assigned. Detailed assignment of the IR absorption bands is provided in Tables S1-S4 in the Supporting Information. For phenol, the assignment obtained is in excellent agreement with the results reported by Michalska et al.[41] The adsorption mode of the methoxyphenol positional isomers was characterised based on the vibrational modes highlighted in Figure 3, which are the stretching vibrations of the alcohol function (ν(OH)), of the aromatic ring (ν(CC)arom), of the C—O bonds involving aromatic C atoms (ν(CO)arom) and of the C—O bond involving the terminal methyl group (ν(CO)aliphat), as well as the in-plane bending of the aromatic CH groups δ(CH). Due to the rigidity of these aromatic molecules, more than one molecular bond may contribute significantly to a dipole moment change and had to be considered for the assignment. Furthermore, except for the ν(OH) mode, the dipole moment changes of these major vibrational modes are all oriented along the plane of the molecule in the gas-phase, but the molecular scaffold may be slightly distorted upon adsorption.

A major difference for the surface interaction of the four phenols was observed in the higher frequency region of the spectra (4000 – 2800 cm^{-1}). Adsorbed phenol (Figure 3A) and 2-methoxyphenol (Figure 3B) gave rise to a broad ν(OH) absorption band revealing that the alcohol bond of these detected surface phenols was weakened but remained intact at the catalytic solid-liquid interface. In contrast, 3-methoxyphenol (Figure 3C) and 4-methoxyphenol (Figure 3D) featured a broad ν(OH) absorption band in dissolution, but not in the presence of the catalyst. In liquid solution, both 3- and 4-methoxyphenols form intermolecular hydrogen-bonds involving the phenolic and methoxy group. Nonetheless, the intermolecular H-bonding is broken upon adsorption on the catalyst. The adsorption of 3-methoxyphenol and 4-methoxyphenol on the catalyst was evident from the absorption bands in the mid frequency region (1850 – 950 cm^{-1}), and the absence of any ν(OH) vibration indicates the predominant formation of the corresponding methoxyphenolates at the catalytic solid-liquid interface.

According to the surface selection rule,[40] IR signals belonging to a dipole moment change of a bond oriented parallel to paramagnetic RANEY® Ni would be inexistent. Therefore, detection of strong ν(CC)arom and ν(CO)arom absorption revealed that the aromatic ring system and the two in-plane C—O bonds of these surface methoxyphenolates are considerably tilted. To understand the selectivity of the catalytic systems towards C—O bond cleavage, it is particularly crucial to gain information on the C—O methoxy bond of adsorbed methoxyphenols. In the ν(CO)arom stretch region in Figure 3D, the rather broad absorption band of the dissolved 4-methoxyphenol centred at 1235 cm^{-1} was split into two distinct peaks at 1227 and 1218 cm^{-1} upon adsorption. Based on our gas-phase DFT calculations, these two bands cannot be assigned unambiguously to two distinct C—O bonds. However, considering the formation of a surface phenolate, it can be inferred that the phenoxy C—O bond of adsorbed 4-methoxyphenolate is weakened and we assign the band at 1218 cm^{-1} to the alkoxide C—O bond. On the other hand, the higher-frequency band at 1227 cm^{-1} could be attributed to the methoxy C—O stretch. The negligible red-shift of this vibrational mode indicates that the strength of this C—O bond is rather unaffected by the adsorption onto the catalyst, and accordingly the *para*-methoxy substituent would be located away from the surface. As seen in Figure 3C, the ν(CC)arom absorption band of adsorbed 3-methoxyphenol at 1285 cm^{-1}, which can be specifically assigned to the methoxy C—O bond, was not shifted compared to dissolved 3-methoxyphenol. Therefore, we propose that, in the predominant surface orientation of 3-methoxyphenol and 4-methoxyphenol, the methoxy bond is not interacting with the catalyst. This feature explains the low

selectivity towards C—O bond cleavage observed for these two substrates.

Regarding the adsorption of 2-methoxyphenol on RANEY® Ni, the surface spectrum (Figure 3B) shows not only different spectral features in the ν(OH) absorption but also in the mid frequency region (1850 – 950 cm^{-1}). Similar to the surface spectrum of phenol, the ν(C=C)arom bands were significantly attenuated upon adsorption onto the catalyst, with the ν(C=C)arom band at 1493 cm^{-1} being clearly discernible. In addition, the absorption modes of the C—O bond stretch vibrations were nearly completely attenuated, and the spectral features at 1285, 1255 and 1212 cm^{-1} were hardly discerned. Owing to the absence of a C—O stretch vibration, adsorbed 2-methoxyphenol has to adopt a predominant surface configuration characterised by a rather flat adsorption of the aromatic ring and a nearly parallel orientation of the methoxy group. Such an adsorption configuration would allow for a stronger interaction between the methoxy C—O bond and the catalyst surface, which can explain the higher affinity of the 2-methoxy substituent towards DMO. Based on the spectroscopic surface characterisation, we propose the predominant adsorption geometries depicted in Scheme 2. In addition to the interpretation above, the aliphatic C—O bond must be oriented rather parallel to the surface for all methoxyphenols, for the DMO to take place.

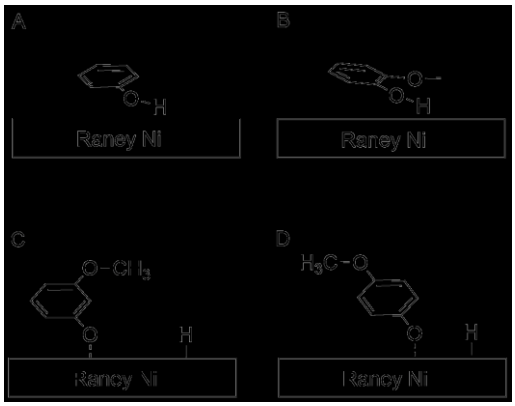

Scheme 2. Proposed adsorption of phenol (A), *ortho*-methoxyphenol (B), *meta*-methoxyphenol (C) and *para*-methoxyphenol (D) on RANEY® Ni from the liquid solution.

The characterization of predominant adsorption geometries by ATR-IR spectroscopy agrees with the entropies of the transition state estimated for the 2-, 3- and 4-methoxyphenols. Enthalpies and entropies of activation (Table 3) were determined for the conversion of the positional isomers, by applying the Eyring-Polanyi equation to the reaction rates obtained at different temperatures (Supporting Information, Figure S3). While enthalpies of the transition states are similar for all substrates (as also previously noticed for the energy of activation), entropy estimated for the 2-methoxyphenol is slightly smaller than those for the other two positional isomers. This observation is consistent with the 2-methoxyphenol flat adsorption on the surface of catalyst. Indeed, when a molecule adsorbs onto a surface in a more planar geometry, a greater decrease of the entropy should be expected, due to the reduction of its molecular motion.[42]

Table 3. Kinetic parameters based on the Eyring–Polanyi equation for the H-transfer conversion of 2-methoxyphenol (2-MeOPh), 3-methoxyphenol (3-MeOPh) and 4-methoxyphenol (4-MeOPh).

Parameters	2-MeOPh	3-MeOPh	4-MeOPh
$\Delta H^{\ddagger}$ (kJ mol^{-1})	71.7±3.3	76.9±2.6	76.1±3.6
$\Delta S^{\ddagger}$ (J mol^{-1} K^{-1})	-75.4±6.0	-64.2±3.7	-66.5±5.3

Experimental

H-Transfer reactions

Substrate (1.8 mmol), n-hexadecane (internal standard for GC analysis, 0.1 mmol), RANEY® Ni 2800 (1.0 g, washed with three 5-mL portions of 2-PrOH to remove water), 2-PrOH (6 mL) and a magnetic stirrer were placed in a 20-mL glass vial. The vial was flushed with Ar and then tightly sealed. The experiment was performed under magnetic stirring (800 rpm) at 80 or 120°C for 2 h. Aliquots of the reaction mixture were taken at the indicated times.

Hydrogenation

In a 45-mL pressure vessel reactor, substrate (1.8 mmol), n-hexadecane (0.1 mmol, internal standard for GC), RANEY® Ni 2800 (1.0 g, washed with three 5-mL portions of 2-methyltetrahydrofuran to remove water), 2-MeTHF (6 mL) and a magnetic stirrer were introduced. The system was flushed with H_2 twice and then pressurised with 40 bar of H_2. The experiment was performed under magnetic stirring (800 rpm) at 120°C for 2h.

GC analysis

The samples were analysed by GC using a Shimadzu QP2010 Plus gas chromatograph, equipped with a ZB-1HT Inferno column (30 m, 0.25 mm ID, df 0.25 µm). The injector temperature was 340°C. The temperature program started at 40°C, followed by an increase of the temperature at a rate of 15 °C min^{-1} to 170°C and then increase again at 60 °C min^{-1} to an isothermal step at 300°C for 5 min. The compounds were identified comparing the EI-MS spectrum with the MS libraries NIST 08, NIST 08s, and Wiley 9. The quantification was performed using the response of the FID.

ATR-IR spectroscopic measurements

The *in-situ* ATR-IR spectroscopic measurements were performed using a custom-built setup, which is described in detail in the literature.[43] A thin film of Raney Ni was deposited onto a ZnSe crystal under Ar atmosphere by shaking a hexane solution containing Raney Ni and pouring the suspension into a form as described in reference.[43] The film was then sealed into the ATR-IR spectroscopic flow-through cell under Ar

atmosphere and transferred to the continuous flow setup.[43] The Ar was removed from the cell with a cyclohexane solution at a flow rate of 0.5 mL min^{-1}, after which the flow rate was increased to 2.7 mL min^{-1}. A background spectrum was collected under a flow of cyclohexane at a flow rate of 2.7 mL min^{-1}. For the adsorption experiments, the film was treated with a cyclohexane solution containing 1 mM of the molecule of interest and an ATR-IR spectrum was recorded every 20s. Afterwards, the cell was again flushed with cyclohexane to remove dissolved species, which allowed detecting only adsorbed species. Dissolution spectra were collected following the same procedure on a blank crystal in the absence of the catalyst film.

DFT calculations

The molecular geometry of phenol and the methoxyphenols was optimised using the gas-phase B3LYP/def2-SV(P) method as implemented in Turbomole 6.3.[44] The optimised structure was confirmed as minima by a full gas phase frequency calculation. Vibrational modes were calculated within the harmonic approximation using gas-phase frequency calculations.

Conclusions

We have demonstrated that the interaction established between the methoxyphenol positional isomers and the RANEY® Ni determines their reactivity pattern towards H-transfer reactions. In fact, 2-methoxyphenol predominantly undergoes demethoxylation. On the other hand, for 3- and 4-methoxyphenols hydrogenation of the aromatic ring is the dominant reaction. Particularly for 2-methoxyphenol, the DMO preference over HYD is very interesting as it also deviates from the typical reactivity pattern found in conventional hydrogenation under H_2 pressure. Apparently, under H_2 pressure, the planar adsorption through the aromatic ring is less favoured, reducing the population of phenolic species with the methoxy group orientated parallel to the catalyst surface. As a result, DMO becomes less dominant leading to a product mixture of cyclohexanol and 2-methylcyclohexanol (54:46). For *meta*- and *para*-isomers, tilted adsorption of methoxyphenol via the formation of a phenolate surface species prevents the alignment of the C—O bond of the methoxyl group parallel to the surface, thus hindering the DMO pathway.

The current findings present an alternative explanation to previously reported enol-keto tautomerisation mechanism,[45-47] rationalising the preference of 2-methoxyphenol to undergo DMO rather than direct phenol dehydroxylation despite the similar bond dissociation enthalpy for both C—O bonds in $C6H_5$-OCH_3 and C_6H_5-OH. This means that this tautomeric mechanism, in which cleavage of C(sp^3)-O bonds prevails over the partial hydrogenation of the ring and the direct C(sp^2)-O cleavage due to the lower activation energy required, does not need to be primarily invoked to elucidate the product distribution for each positional isomer of methoxyphenol obtained from H-transfer reactions.

In a broader context, this fundamental knowledge on how to direct product selectivity based on molecular understanding of interactions between substrate and catalyst surface is of extreme importance for the biorefinery concept. In fact, it contributes to the design of catalysts for the target production of value-added chemicals in which the problem posed by the formation of (complex) product mixtures must be alleviated, in order to improve the atom-economy of the overall process chains.

Conflict of interest

There are no conflicts to declare.

Acknowledgements

R.R. acknowledges the financial support provided by the ERC Consolidator Grant (LIGNINFIRST, Project Number: 725762).

Notes and references

1 J. Su, L. Yang, X. Yang, M. Lu, B. Luo and H. Lin, *ACS Sustain. Chem. Eng.*, 2015, **3**, 195.
2 X. Tang, L. Hu, Y. Sun, G. Zhao, W. Hao and L. Lin, *RSC Adv.*, 2013, **3**, 10277.
3 M. von Arx, M. Wahl, T. A. Jung and A. Baiker, *Phys. Chem. Chem. Phys.*, 2005, **7**, 273.
4 R. Rinaldi, *Catalytic Hydrogenation for Biomass Valorization*, Royal Society of Chemistry, 2014.
5 M. J. Gilkey and B. Xu, *ACS Catal.*, 2016, **6**, 1420.
6 X. Wang and R. Rinaldi, *Energy Environ. Sci.*, 2012, **5**, 8244.
7 J. Geboers, X. Wang, A. B. de Carvalho and R. Rinaldi, *J. Mol. Catal. A: Chem.*, 2014, **106**, 388.
8 D. Wang and D. Astruc, *Chem. Rev.*, 2015, **115**, 6621.
9 P. Ferrini and R. Rinaldi, *Angew. Chem. Int. Ed.*, 2014, **53**, 8634.
10 R. Rinaldi, R. Jastrzebski, M. T. Clough, J. Ralph, M. Kennema, P. C. A. Bruijnincx and B. M. Weckhuysen, *Angew. Chem. Int. Ed.*, 2016, **55**, 8164.
11 M. V. Galkin and J. S. M. Samec, *ChemSusChem*, 2016, **9**, 1544.
12 P. Ferrini, C. A. Rezende and R. Rinaldi, *ChemSusChem*, 2016, **9**, 3171.
13 G. Calvaruso, J. Burak, M. T. Clough, M. Kennema, F. Meemken and R. Rinaldi, *ChemCatChem*, 2017, **9**, 2627.
14 R. C. Mebane, K. L. Holte and B. H. Gross, *Synth. Commun.*, 2007, **37**, 2787.
15 Z. Yang, Y.-B. Huang, Q.-X. Guo and Y. Fu, *Chem. Commun.*, 2013, **49**, 5328.
16 M. Kim, J.-M. Ha, K.-Y. Lee and J. Jae, *Catal. Comm.*, 2016, **86**, 113.
17 T. Guo, Q. Xia, Y. Shao, X. Liu and Y. Wang, *Appl. Catal. A: Gen.*, 2017, **547**, 30.
18 X. Besse, Y. Schuurman and N. Guilhaume, *Appl. Catal. B: Environ.*, 2017, **209**, 265.
19 H. Wu, J. Song, C. Xie, C. Wu, C. Chen and B. Han, *ACS Sust. Chem. Eng.*, 2018, 10.1021/acssuschemeng.7b02993.
20 Y. N. Regmi, J. K. Mann, J. R. McBride, J. Tao, C. E. Barnes, N. Labbé and S. C. Chmely, *Catal. Today*, 2018, **302**, 190.
21 J. He, S. Yang and A. Riisager, *Catal. Sci. Technol.*, 2018, **8**, 790.
22 Y. Yoon, R. Rousseau, R. S. Weber, D. Mei and J. A. Lercher, *J. Am. Chem. Soc.*, 2014, **136**, 10287.
23 E. Furimsky, *Appl. Catal. A: Gen.*, 2000, **199**, 147.
24 I. Graça, J. M. Lopes, H. S. Cerqueira and M. F. Ribeiro, *Ind. Eng. Chem. Res.*, 2013, **52**, 275.
25 S. Liu, H. Wang, K. J. Smith and C. S. Kim, *Energy Fuels*, 2017, **31**, 6378.

26 J. Huang, X. Li, D. Wu, H. Tong and W. Li, *J. Renew. Sustain. Energy*, 2013, **5**, 043112.
27 C.-c. Chiu, A. Genest, A. Borgna and N. Rösch, *ACS Catal.*, 2014 **4**, 4178.
28 K. Lee, G. H. Gu, C. A. Mullen, A. A. Boateng and D. G. Vlachos, *ChemSusChem*, 2015, **8**, 315.
29 J. Lu, S. Behtash, O. Mamun and A. Heyden, *ACS Catal.*, 2015, **5**, 2423.
30 W. Song, Y. Liu, E. Baráth, C. Zhao and J. A. Lercher, *Green Chem.*, 2015, **17**, 1204.
31 G. Brieger and T. J. Nestrick, *Chem. Rev.*, 1974, **74**, 567.
32 B. H. Gross, R. C. Mebane and D. L. Armstrong, *Appl. Catal. A: Gen.*, 2001, **219**, 281.
33 X. Wang and R. Rinaldi, *ChemSusChem*, 2012, **5**, 1455.
34 H. Bu, P. Bertrand and J. W. Rabalais, *J. Chem. Phys.*, 1993, **98**, 5855.
35 L. Delle Site, A. Alavi and C. Abrams, *Phys. Rev. B*, 2003, **67**, 193406.
36 C.-c. Chiu, A. Genest, A. Borgna and N. Rösch, *Phys. Chem. Chem. Phys.*, 2015, **17**, 15324.
37 L. M. Ghiringhelli, R. Caputo and L. Delle Site, *Phys. Rev. B*, 2007, **75**, 113403.
38 J. A. Ruiz-Santoyo, M. Rodriguez-Matus, J. L. Cabellos, J. T. Yi, D. W. Pratt, M. Schmitt, G. Merino and L. Álvarez-Valtierra, *J. Chem. Phys.*, 2015, **143**, 094301.
39 M. Kennema, I. B. D. de Castro, F. Meemken and R. Rinaldi, *ACS Catal.*, 2017, **7**, 2437.
40 R. G. Greenler, D. R. Snider, D. Witt and R. S. Sorbello, *Surf. Sci.*, 1982, **118**, 415.
41 D. Michalska, W. Zierkiewicz, D. C. Bieńko, W. Wojciechowski and T. Zeegers-Huyskens, *J. Phys. Chem. A*, 2001, **105**, 8734.
42 J. Gaberle, D. Z. Gao, M. B. Watkins and A. L. Shluger, *J. Phys. Chem. C*, 2016, **120**, 3913.
43 F. Meemken, P. Muller, K. Hungerbuhler and A. Baiker, *Rev. Sci. Instrum.*, 2014, **85**, 84101.
44 *Turbomole V6.2 2010*, a development of University of Karlsruhe and Forschungszentrum Karlsruhe GmbH, 1989-2007.
45 P. M. de Souza, R. C. Rabelo-Neto, L. E. P. Borges, G. Jacobs, B. H. Davis, T. Sooknoi, D. E. Resasco and F. B. Noronha, *ACS Catal.*, 2015, **5**, 1318.
46 L. Nie and D. E. Resasco, *J. Catal.*, 2014, **317**, 22.
47 L. Nie, P. M. de Souza, F. B. Noronha, W. An, T. Sooknoi and D. E. Resasco, *J. Mol. Catal. A: Chem.*, 2014, **388-389**, 47.